Surface morphology characterisation for parts produced by the high speed selective laser melting

IOP Conf. Series: Materials Science and Engineering **655** (2019) 012045 doi:10.1088/1757-899X/655/1/012045

Surface morphology characterisation for parts produced by the high speed selective laser melting

M Shange[1, 2], I Yadroitsava [2], S Pityana[1], I Yadroitsev[2], and D Bester[1]

[1] Laser Enabled Manufacturing, National Laser Centre, CSIR, Pretoria, 0001, South Africa.

[2] Department of Mechanical Engineering, Central University of Technology, Free State 9301, South Africa

E-mail: mshange@csir.co.za

Abstract. Additive Manufacturing (AM) systems are unique in terms of fast production and lead time to market. South Africa has built the AM Laser Powder Bed Fusion (LPBF) machine called Aeroswift with the world's largest build volume and highest speed. Surface roughness of LPBF parts depends on process-parameters. High surface roughness and deformations during processing limit the application of this technology for certain industrial applications that require high precision. This study characterises the surface roughness for self-supported parallelepipeds samples produced using the Aeroswift platform. Test artefact parallelepipeds were built with 0-90 degrees sloping angles with respect to the building direction. Surface roughness for the as-built samples was analysed using Mitutoyo SURFTEST SJ-210 system and Zeiss Smartzoom 5 digital microscope. It was found that roughness values were higher for the bottom surfaces (overhang part) compared to upward surfaces, as expected. This was attributed to the higher amount of attached partially melted powder particles that were observed on the downward surface. Absolute values of *Ra* and *Rz versus* scanning direction and slope angle were found and analysed.

1. Introduction

Additive manufacturing (AM) is described by ASTM F2792 as a method of joining materials to create parts from 3-D model data with a layer-by-layer process as opposed to conventional techniques, also the 3D printing term is often used synonymously with additive manufacturing [[1]]. Laser powder bed fusion (LPBF) or selective laser melting, direct metal laser sintering and LaserCusing are AM processes that use a laser to consolidate powder material to create a 3D object. The melting of consecutive layers of powder is achieved through the laser beam energy. Moreover, standard metallic powders that melt completely are used, thus ensuring the mechanical properties match 100 percent density or even beat conventional techniques [[2]]. LPBF is a layer by layer manufacturing technique therefore complex geometries can be produced [[3]]. Furthermore, the complexity of the product does not increase the cost [[4]]. However, the more complex the part the more difficult it is to carry-out post processing treatment [[5]]. The common types of post processing: include support structure removal, improving surface finish, post heat treatment etc. Bremen *et al.* [[2]] stated that improving the surface finish is the most costly of the post processing treatments of LPBF parts. Due to the growing interest for parts manufactured by LPBF, it is important to define limitations at an earlier phase of design [[6]]. Therefore,

designers for AM are encouraged to possess a quality control or inspection tool to predict the level of the resulting surface roughness before parts are manufactured. The proposed tools include fabricating test artefacts with varying angles to characterise different surfaces topographies. Commonly used test artefacts comprise parallelepipeds, truncheons etc. Figure 1 shows one example of a test artefact.

Figure 1: Truncheon test artefacts studied by Strano et al [[7]]

Covarrubias and Eshraghi [[5]] conducted a study on two different types of test artefacts: parallelepipeds and cubes with varying angles. The cubes had inclinations of 45°, 60°, 75° and 90°. The parallelepipeds had of seven rectangular cubes with angles from 0° to 90° with a 15° increment between the angles. Similarly, Strano *et al.* [[7]] investigated surface texture on a truncheon with sloping angles from 0° to 90° with a 5° increment between the angles. Barari *et al*. [[8]] performed a study on cusp geometry with different angles. These studies found that a decrease in angle towards the base-plate is associated with increased surface roughness. Also the downward facing surfaces for overhanging objects have been identified to possess a poor surface quality than upward surfaces. Similarly, it was found that surface quality improves as the sloping angle increases from the base plate.

Authors did not give a distinct difference in the roughness for the two surfaces, downskin and upskin. The downskin is defined as the downward facing surface whereas upskin is defined as the upwards facing surface. However, this study seeks to address the difference between the two surfaces for as built Ti6Al4V samples of parallelepipeds, with angles from 25° to 90° shown in Figure 2. This will be achieved by comparing the arithmetic mean average (*Ra*) and ten-point height (*Rz*) as a function of an angle for both upskin and downskin surfaces.

2. Materials and Methods

2.1. Materials characterization

All samples were fabricated using gas atomised pre-alloyed Ti6Al4V (grade 5) powder. Ti6Al4V amongst all the titanium grades is the widely used alloy due to its good mechanical properties [[9]]. Furthermore, parts that are manufactured with Ti6Al4V are lightweight which makes it ideal for aerospace application. The powder used to build the samples is supplied by TLS Technik and has a powder distribution of 20 to 60 µm. The chemical composition for the Ti6Al4V is shown in Table 1.

Table 1: Chemical composition of employed Ti6Al4V powder.

Al	V	C	Fe	O	N	H	Y	Zn	Sn	Ti
6..8%	3.96%	0.006%	0.161%	0.087%	0.008	0.002	< 0.01	< 0.002	<0.004	balance

2.2. Methods

Before the building process the powder was dried at 120°C in an oven for 3-4 hours to remove moisture. During processing, an inert argon atmosphere was used to avoid oxidation and the amount of oxygen was maintained below 500 ppm. Layer thickness was maintained at 50 µm which is the distance equated to the movement of the z-axis. To build the samples, bi-directional scanning strategy was used. The Aeroswift platform uses the ytterbium laser with a wavelength of 1076 nm and a maximum power output

of 5 kW. This machine has a build volume of 2000 mm × 600 mm × 600 mm. After completing the building process, samples were submerged in an ultrasonic-bath for 10 minutes in water. The surface roughness for the samples was measured according to ISO 427:1997 [[10]] using a Mitutoyo Surftest SJ-210. The samples were measured in the as-built condition, meaning no surface finishing was conducted. The stylus, which is the measuring tip of the instrument, was made to traverse perpendicular to the scanning direction to account for the stair-stepping effect. Scanning direction is described in [[7]] as a direction in which the laser traverses, and [[5]] defines that stair effect occurs as a result of additive manufacturing layer by layer fabrication process. Roughness parameters *Ra* and *Rz* in [[11]] can be represented as follows:

$$Ra = \frac{1}{l}\int_0^l |y(x)|\, dx \qquad (1)$$

$$Rz = \frac{1}{n}\left(\sum_{i=1}^{n} p_i - \sum_{i=1}^{n} v_i\right) \qquad (2)$$

Where l is sampling length, p_i is vertical distance from the highest peak and v_i the lowest valley within five sampling lengths. Ten-point height (*Rz*) evaluates the average value of five highest peaks and five lowest valleys within the measured sampling length [[11]]. The sampling length that was used is 2.5 mm based on the standard [[10]]. Subsequently, a non-contact 3D Zeiss Smartzoom 5 digital microscope was used to validate and evaluate surface morphology. The tested samples had angles from 25° to 90° with a 5° increment.

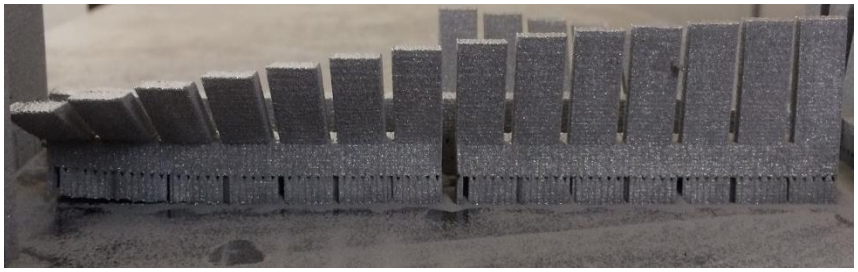

Figure 2: Fabricated test artefact parallelepipeds samples showing angles from 25° to 90° (left to right)

3. Experimental Results and Discussions

3.1. Surface roughness characterization:

A total of 14 upskin surfaces and 14 downskin surfaces were tested and data for these surfaces were measured in three different places for each surface and averaged. The profile of the resulting surface roughness (*Ra*) for both downskin and upskin surfaces as a function of building angle for parts manufactured on the Aeroswift platform are represented in Figures 3 and 4, respectively.

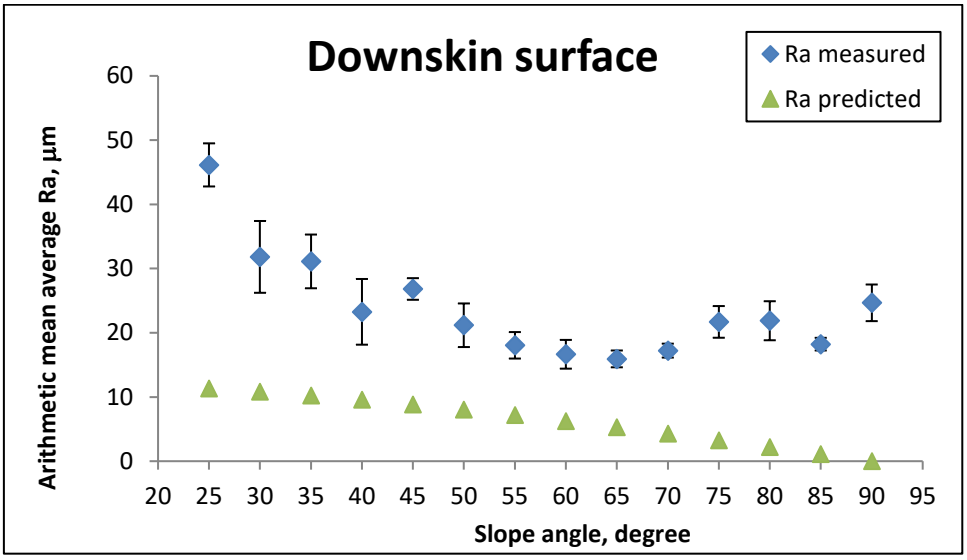

Figure 3: *Ra* values for downward facing surfaces

As expected, it can be seen from Figure 3 that angle 25° had the highest roughness value of all the manufactured angles of 46.4 µm which is a significant amount. This is a result of un-melted powder particles that adhere to the surface of the part during processing especially when the build angle is low (25°). This can be supported by the image in Figure 6(a), which shows high peaks representing unevenness of the surface. According to Triantaphyllou *et al.* [[12]] the increased roughness for downskin surfaces is a result of gravity and capillary forces where the melt pool sags into the un-melted powder particles. As the melt pool solidifies, it causes the surrounding un-melted powder particles to attach on the surface thereby increasing roughness. Furthermore; poor surface roughness at lower angles was found to be a result of the stair stepping effect as previously reported by Covarrubias and Enshragi [5], Barari *et al.* [[8]] and Kaji and Barari [[13]]. As observed from the results a 65° angle generated a better surface quality than all other angles. This can be confirmed by the low peaks as seen in the Figure 6c. This is because in LPBF as the sloping angle increases from the base plate it is associated with better staircase effect. This confirms a similar trend that was observed by Strano *et al.* [[7]] where it was found that better surface quality can be achieved at the angle of 75° as opposed to 90°. On the other hand, Covarrubias and Enshragi [[5]] showed that the *Ra* and *h (Rz)* values in AM can be predicted according to the analytical equation presented by:

$$h = \frac{L_t}{\sin(\propto)} \quad (3)$$

$$Ra\ predicted = \frac{L_t \sin(\alpha)}{4\tan(\alpha)} \quad (4)$$

Where h is the distance between consecutive step edges, L_t is the layer thickness, and $\propto$ is the inclined angle. This approach was previously used by Reeves and Cobb [[15]] for surface deviation modelling of stereolithography components. The latter equation 4 neglect that LPBF processed parts had round corners, it assumes an ideal environment with perfect sharp edges which make it not ideal for quantifying the degree of surface roughness (Figures 3 and 4). Predicted *Rz* values (Figures 5a and b) were calculated taking into account about 50% shrinkage of powder material and 50 µm distance equated to the movement of the z-axis (see equation 3).

According to the measured roughness values seen in Figure 4, initially the roughness value increase from 25° to 35 °and subsequently formed a zig-zag profile until 90°. From the graph it can be deduced that both 75° and 35° had the highest peaks whereas angle 85° had the lowest *Ra* value of 19,5 µm.

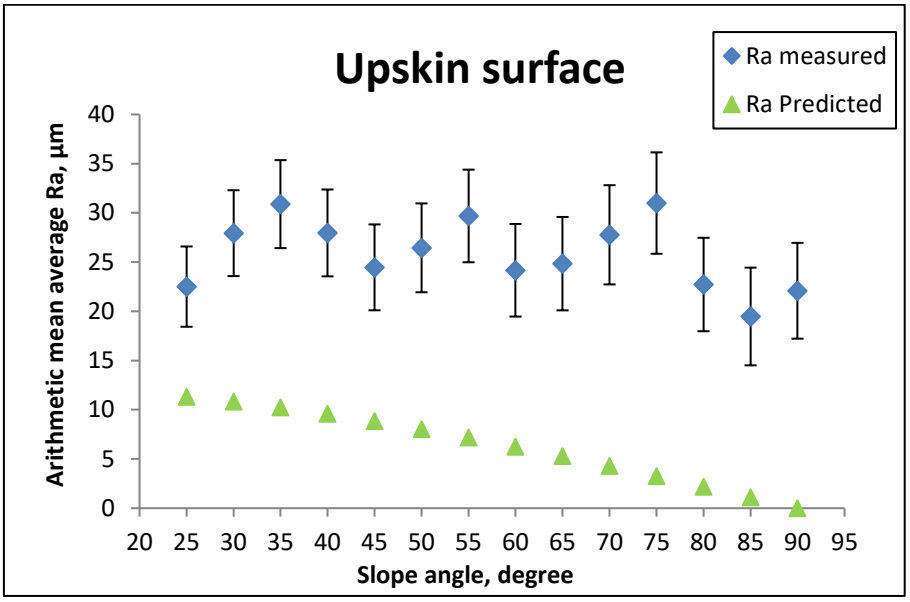

Figure 4: *Ra* values for upward facing surfaces

Since *Ra* is the mean value of the whole profile, *Rz* values also were investigated to analyse individual peaks and valleys (Figure 5a and b). The qualitative analysis for angle 25°, 65° and 90° are represented in Figure 6(b) (d) (f) below for comparison with the previous trend in Figure 4. The melt pool for the top surface does not directly solidify on top of the un-melted powder as in the case of the downskin as previously mentioned. The zig-zag trend might be aggravated by stair-stepping effect especially for smaller sloping angles wherein as the angle increases partially sintered powder particles contributed to the higher roughness. It is well known in literature that angles less than 45 degrees are greatly influenced by stair stepping effects [[5]]. This type of profile has been defined by Strano *et al.* [[7]] and Krol and Tanski [[14]] who stated that the amount of powder concentration of un-melted particles sticking on the edges increases as the inclination angle rises towards the vertical direction. Furthermore, because at low angles the particle size is smaller than the step edges, as the angle increases the edges become smaller thus leading to a higher concentration of partially sintered particles thus resulting in an increased poor surface quality.

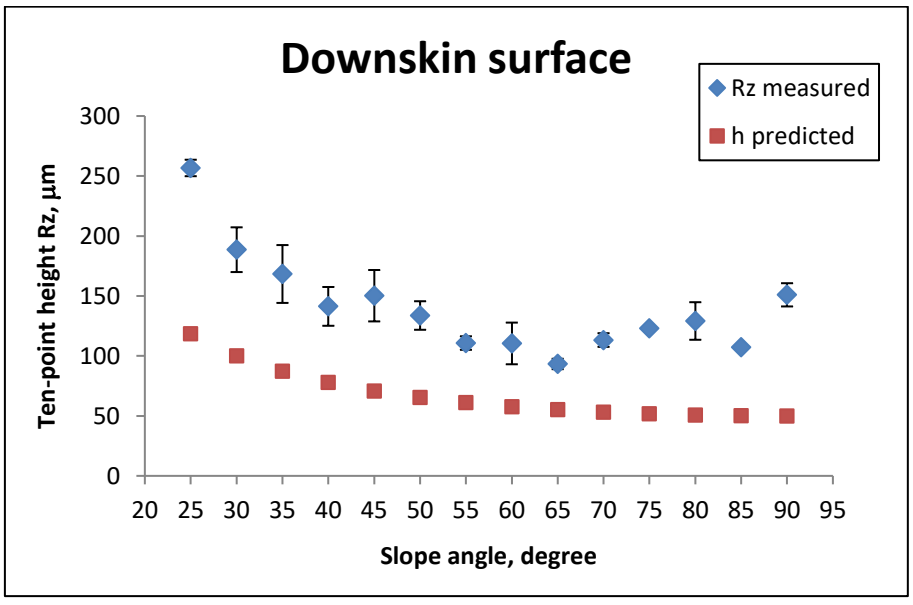

(a)

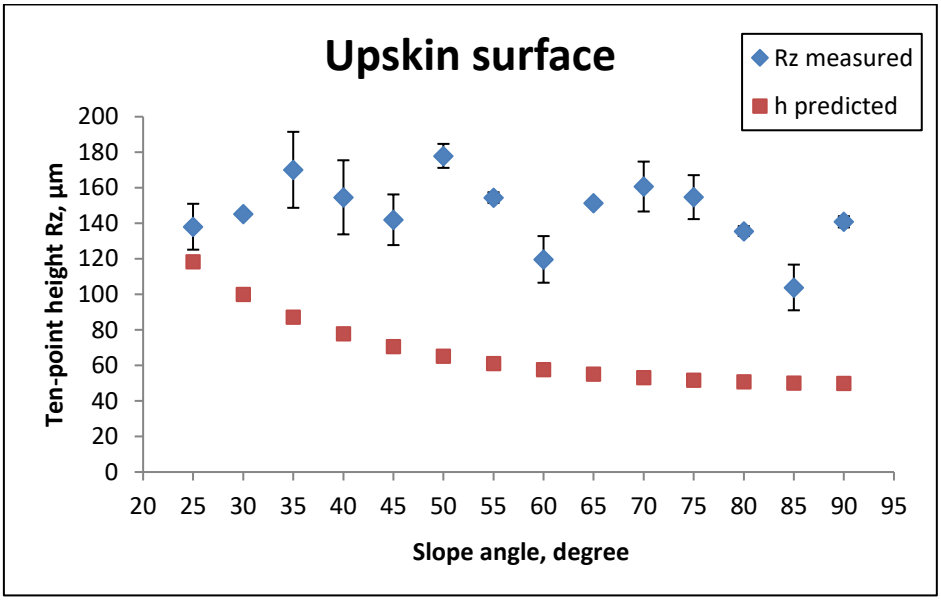

(b)

Figure 5: *Rz* values for downward (a) and upward (b) facing surfaces.

3.1.1. Qualitative analysis of surface roughness

Figure 6 (a) to (f) show the difference between the downward facing surface on the left and the upward facing surface on the right. As it can be seen, the noticeable difference from the 3D images is from the downskin surfaces comprised of large peaks compared to upskin surfaces. Furthermore the samples on the downskin showed greater irregularities or unevenness on to their surface.

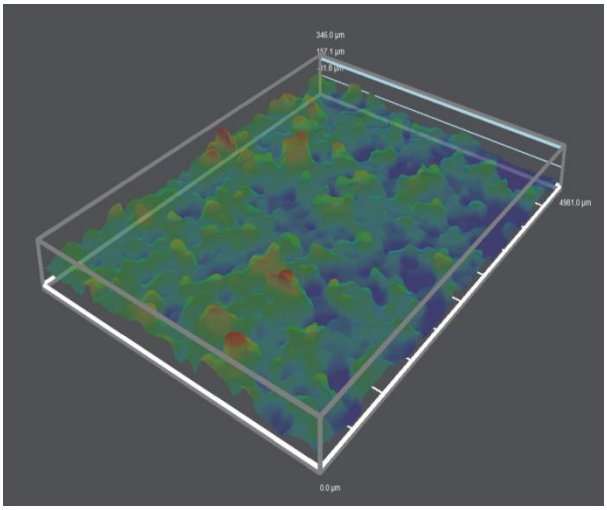

a) 25° angle downskin

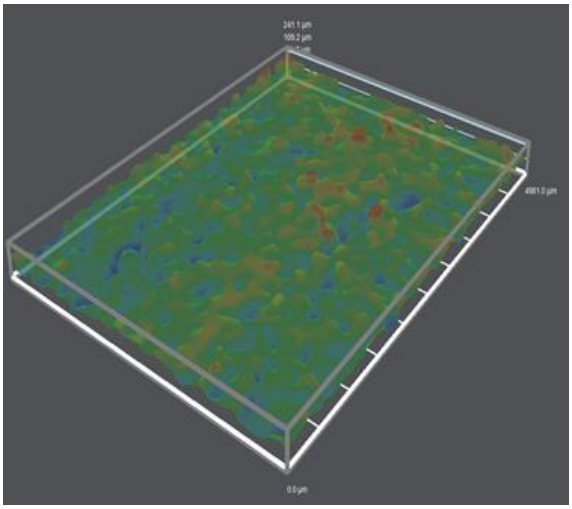

b) 25° angle upskin

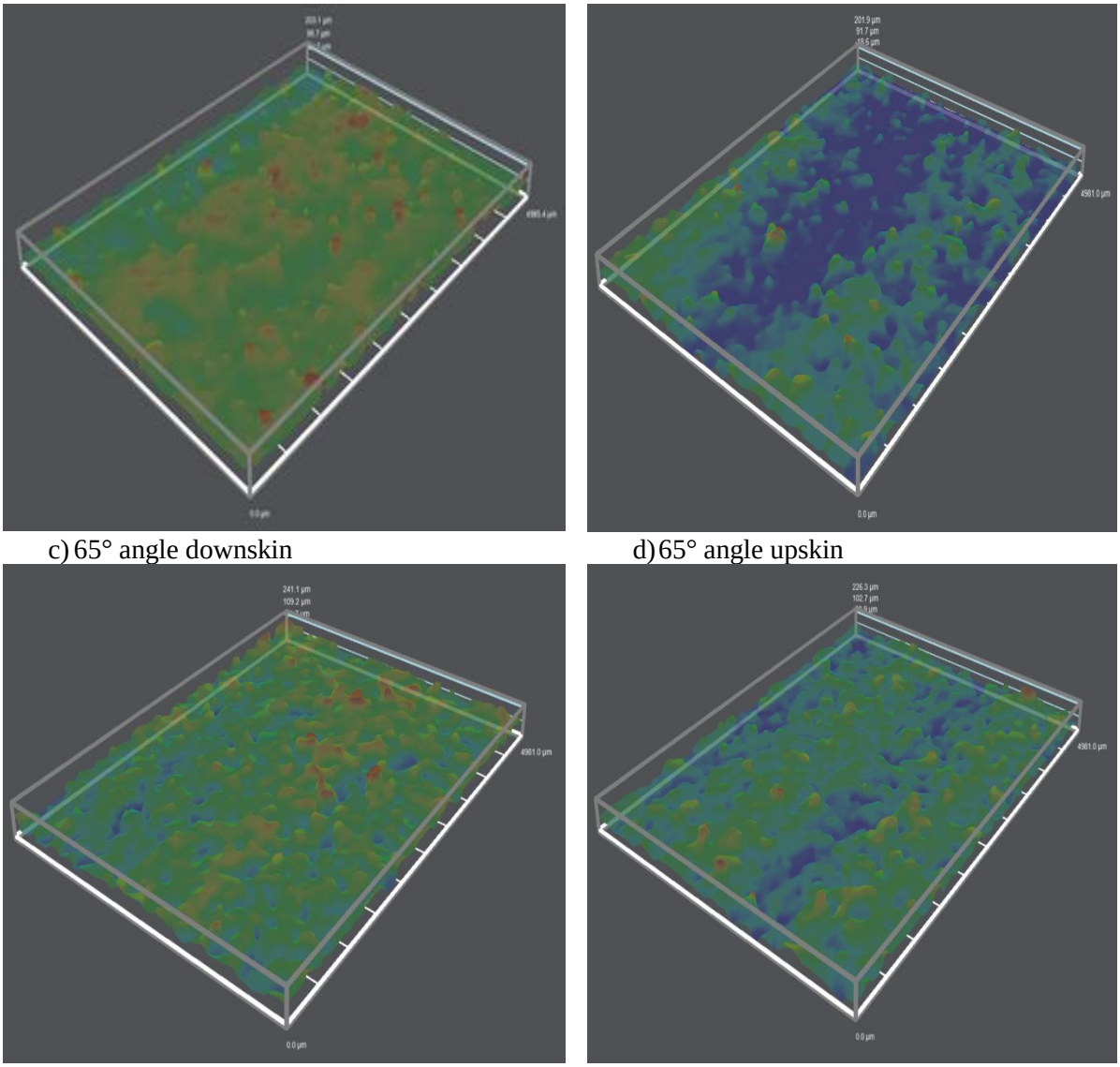

c) 65° angle downskin d) 65° angle upskin

e) 90°angle downskin f) 90° angle upskin

Figure 6: 3D surface reconstructions by optical microscope for different angles. Blue colour is valleys, red colour is peaks.

4. Conclusion

The aim of this study was to highlight the fundamentals of the level of surface roughness that can be expected on the as-built components produced by the Aeroswift platform. Based on Figure 2, it was determined that better surface roughness of downskin can be achieved when building at angles between 40° and 90°. There were no significant differences in surface roughness of upskin surfaces *versus* slope angle. Thus, upskin surface morphology depends on process parameters and scanning strategy. According to the obtained results, it can be concluded that powder particles and staircase-effect played a key role in the degree of roughness mostly for downskin surfaces. The collected data of the surface roughness is the first step in diagnosing the as-built manufactured component and will advise the suitable angles to use before parts are manufactured by the Aeroswift platform.

Acknowledgments
The Authors would like to extend our thanks to the CSIR – National Laser Centre and to the South African Research Chairs Initiative of the Department of Science and Technology and National Research Foundation of South Africa (Grant №97994) for all their support to this research.

5. References

[1]. ASTM F2792-12a, Standard Terminology for Additive Manufacturing Technologies, (Withdrawn 2015), ASTM International, West Conshohocken, PA, 2012.
[2]. Bremen, S., Meiners, W. and Diatlov, A., 2012. Selective laser melting: a manufacturing technology for the future. Laser Technik Journal, 9(2), pp.33-38.
[3]. Buchbinder, D., Schleifenbaum, H.B., Heidrich, S., Meiners, W. and Bültmann, J., 2011. High power selective laser melting (HP SLM) of aluminum parts. Physics Procedia, 12, pp.271-278.
[4]. Karme, A., Kallonen, A., Matilainen, V.P., Piili, H. and Salminen, A., 2015. Possibilities of CT scanning as analysis method in laser additive manufacturing. Physics Procedia, 78, pp.347-356.
[5]. Covarrubias, E.E. and Eshraghi, M., 2018. Effect of Build Angle on Surface Properties of Nickel Superalloys Processed by Selective Laser Melting. JOM, 70(3), pp.336-342.
[6]. Kranz, J., Herzog, D. and Emmelmann, C., 2015. Design guidelines for laser additive manufacturing of lightweight structures in TiAl6V4. Journal of Laser Applications, 27(S1), p.S14001.
[7]. Strano, G., Hao, L., Everson, R.M. and Evans, K.E., 2013. Surface roughness analysis, modelling and prediction in selective laser melting. Journal of Materials Processing Technology, 213(4), pp.589-597.
[8]. Barari, A., Kishawy, H.A., Kaji, F. and Elbestawi, M.A., 2017. On the surface quality of additive manufactured parts. The International Journal of Advanced Manufacturing Technology, 89(5-8), pp.1969-1974.
[9]. Mathoho, I., 2017. Enhancing the integrity of machined titanium alloy (Doctoral dissertation, University of Johannesburg).
[10]. ISO, E., 1997. 4287–Geometrical Product Specifications (GPS)–Surface Texture: Profile Method–Terms, Definitions and Surface Texture Parameters. International Organization for Standardization: Geneva, Switzerland.
[11]. Gadelmawla, E.S., Koura, M.M., Maksoud, T.M.A., Elewa, I.M. and Soliman, H.H., 2002. Roughness parameters. Journal of materials processing technology, 123(1), pp.133-145.
[12]. Triantaphyllou, A., Giusca, C.L., Macaulay, G.D., Roerig, F., Hoebel, M., Leach, R.K., Tomita, B. and Milne, K.A., 2015. Surface texture measurement for additive manufacturing. Surface Topography: Metrology and Properties, 3(2), p.024002.
[13]. Kaji, F. and Barari, A., 2015. Evaluation of the surface roughness of additive manufacturing parts based on the modelling of cusp geometry. IFAC-PapersOnLine, 48(3), pp.658-663.
[14]. Krol, M. and Tański, T., 2016. Surface quality research for selective laser melting of Ti-6Al-4V alloy. Archives of Metallurgy and Materials, 61(3), pp.1291-1296.
[15]. Reeves, P. E. and Cobb, R. C., 1997. Reducing the surface deviation of stereolithography using in-process techniques. Rapid Prototyping Journal, 3(1), 20–31.